Received: 19 November 2021 | Revised: 28 January 2022 | Accepted: 31 January 2022

DOI: 10.1111/jsr.13567

Journal of Sleep Research

RESEARCH ARTICLE

A calibrated model with a single-generator simulating polysomnographically recorded periodic leg movements

Matteo Italia[1] | Andrea Danani[2] | Fabio Dercole[1] | Raffaele Ferri[3] | Mauro Manconi[4,5,6]

[1]Department of Electronics, Information, and Bioengineering, Politecnico di Milano, Milan, Italy

[2]Dalle Molle Institute for Artificial Intelligence, University of Southern Switzerland, University of Applied Science and Arts of Southern Switzerland, Lugano, Switzerland

[3]Oasi Research Institute – IRCCS, Troina, Italy

[4]Sleep Medicine Unit, Neurocenter of Southern Switzerland, Ospedale Civico, Lugano, Switzerland

[5]Faculty of Biomedical Sciences, Universita della Svizzera Italiana, Lugano, Switzerland

[6]Department of Neurology, University Hospital, Inselspital, Bern, Switzerland

Correspondence
Matteo Italia, Department of Electronics, Information, and Bioengineering, Politecnico di Milano, Milan, Italy.
Email: matteo.italia@polimi.it

Summary

The aim of this study was to assess, with numerical simulations, if the complex mechanism of two (or more) interacting spinal/supraspinal structures generating periodic leg movements can be modelled with a single-generator approach. For this, we have developed the first phenomenological model to generate periodic leg movements in-silico. We defined the onset of a movement in one leg as the firing of a neuron integrating excitatory and inhibitory inputs from the central nervous system, while the duration of the movement was defined in accordance to statistical evidence. For this study, polysomnographic leg movement data from 32 subjects without periodic leg movements and 65 subjects with periodic leg movements were used. The proportion of single-leg and double-leg inputs, as well as their strength and frequency, were calibrated on the without periodic leg movements dataset. For periodic leg movements subjects, we added a periodic excitatory input common to both legs, and the distributions of the generator period and intensity were fitted to their dataset. Besides the many simplifying assumptions – the strongest being the stationarity of the generator processes during sleep – the model-simulated data did not differ significantly, to a large extent, from the real polysomnographic data. This represents convincing preliminary support for the validity of our single-generator model for periodic leg movements. Future model extensions will pursue the ambitious project of a supportive diagnostic and therapeutic tool, helping the specialist with realistic forecasting, and with cross-correlations and clustering with other patient meta-data.

KEYWORDS
leg movement activity, pace maker, polysomnography, restless legs syndrome

1 | INTRODUCTION

Periodic limb movements (PLMs) are involuntary motor events mainly involving legs, characterized by the flexion of toe, foot and knee, occurring during wakefulness (PLMW) and mainly during sleep (PLMS), especially non-rapid eye movement (NREM) sleep. PLMs are a frequent phenomenon, being present in the majority of patients with restless legs syndrome (RLS), and in a significant percentage of patients with other sleep or neurological disorders; they can also be an isolated finding in otherwise healthy subjects, especially after the age of 40 years (Ferri, 2012; Pennestri et al., 2006). PLMs are detected by recording both tibialis anterior muscles by means of surface electromyography in the context of polysomnography (PSG). Based on standard scoring criteria (American Academy of Sleep

Medicine, 2014; Ferri et al., 2016), PLMs consist of a series of at least four consecutive candidate leg movements (CLMs) separated by inter-movement intervals (IMIs; from the onset of a CLM to the onset of the next) in the range of 10–90 s. CLMs are leg movements (LMs) with duration longer than 0.5 s and shorter than 10 s if monolateral; shorter than 15 s if bilateral and composed of at most four LMs with duration within 0.5–10 s. When two (or more) LMs occurring in different legs overlap or are separated (from offset to onset) by an interval shorter than 0.5 s, they are considered as one bilateral LM, otherwise as distinct monolateral movements (Ferri et al., 2016). PLMs might hence involve one or both legs. PLM series are interrupted by either a non-candidate LM or an IMI out of the range 10–90 s.

The severity of PLMS is usually quantified with the PLMS index, which indicates the number of PLMS per hour of recording, and is considered abnormal when it exceeds the value of 15 in adults (American Academy of Sleep Medicine, 2014). Despite still being under debate, PLMS might affect sleep quality for their association with cortical arousals and, in the long term, the cardiovascular system, because of their associated repetitive phasic increases in heart rate and blood pressure (Ferri et al., 2017).

The mechanism and the neuroanatomical pathways behind PLMs are unknown, as well as the origin of their periodicity. In the last two decades, PLMs have become an interesting topic under the magnifying glass of sleep researchers, representing today one of the most intriguing and unsolved mysteries in the field of sleep-related movement disorders. In particular, what most attracts the interest of researchers is the mechanism underlying the periodicity of these motor events, which advocates the existence of a biological "pace maker", whose anatomical location or distribution and structure are, however, unknown.

Differently from PLMW, some fundamental aspects of PLMS are now more clear and well accepted by the scientific community: PLMS are strongly suppressed by low doses of dopamine agonists (DAs; Manconi et al., 2007) and are triggered by dopamine antagonists; PLMS occur also in patients with complete transverse spinal cord lesions, indicating that the spinal cord contains the fundamental network to generate them (Ferri et al., 2015; Salminen et al., 2013); the cortical arousals and the autonomic fluctuations usually accompanying PLMS can persist when PLMS are pharmacologically suppressed (Manconi et al., 2012). The latter aspect is against the existence of a direct causal relationship between PLMS, cortical arousals and autonomic activations. Moreover, taking into account that the temporal association between these oscillating phenomena is lost in a patient with transverse spinal lesion (Ferri et al., 2015; Salminen et al., 2013), it might be postulated that these systems are under the influence of multiple "pace makers" that synchronize with each other by a reciprocal and dynamic drag effect (Ferri, 2006).

To solve the puzzle of PLMs is not a sterile exercise of speculative minds, but has potential implications for the clinical practice, especially on the fundamental decision to treat PLMs or not (Figorilli et al., 2017). Moreover, a significant part of the current understanding comes from the use of animal models (Allen et al., 2017), so that an in-silico PLM model would have indisputable advantages from both the ethical and economic viewpoints. The primary aim of this study was to assess, with numerical simulations, if the complex mechanism of two (or more) interacting spinal/supraspinal structures generating PLMs can be explained with a single-generator approach, i.e. by a model calibrated on subjects without PLMs with the only addition of a single periodic excitatory generator.

Our model is the first generating LMs in-silico. However, it is functional to the aim of the study, and therefore preliminary for clinical applications. First of all, it is a phenomenological model, hence describing the LM phenomenon, not the underlying neurophysiology. But more importantly, it assumes, for simplicity, the stationarity of the involved neurological processes, which are known to significantly vary during the sleep cycle and along the night.

2 | METHODS

2.1 | The model

With the aim of designing a phenomenological model of PLMs, we simplified the underlying physiology and assumed that each leg is controlled by a single motor neuron, representative of the central nervous system (CNS) complex pathways, ultimately determining contractions of the leg muscles. This hypothesis may seem drastic, but indeed the PSG recordings are sensitive only to a few motor neurons and measure their average activity, which we describe qualitatively with a single virtual neuron. The two neurons were mathematically described by the well-known Stein model of an integrate-and-fire neuron (Stein, 1965; see Section S1 for a technical description; see Burkitt, 2006, for a review on integrate-and-fire neuron models).

The integrate-and-fire mechanism is quite simple. The neuron state is characterized by its membrane potential, which evolves according to the neuron's synaptic inputs. Excitatory/inhibitory inputs increase/decrease the potential, while a time constant τ rules the potential decay toward a resting value V_0 in the absence of inputs (charge leakage). When the membrane potential reaches a threshold V_{th}, an output spike is generated – the firing of the neuron – which causes the potential to reset at a basal value that, for simplicity, we set to coincide with the resting value V_0. The output spike represents, in our model, the LM onset, while the duration of the movement is obtained from a distribution fitted on clinical data (see 'Calibration').

As schematically represented in Figure 1, each of the two neurons (with membrane potentials $v_L(t)$ and $v_R(t)$ at time t) receives excitatory/inhibitory inputs from the physiological activity of the CNS (physiological inputs in the following), a proportion p of which equally affect both legs (common inputs; magenta in the figure), while the remaining fraction $(1 - p)$ is leg-specific (left and right inputs; red and blue, respectively). For subjects showing significant PLMs, we added a periodic input common to both legs, representing our single periodicity generator (gold). The period and intensity of

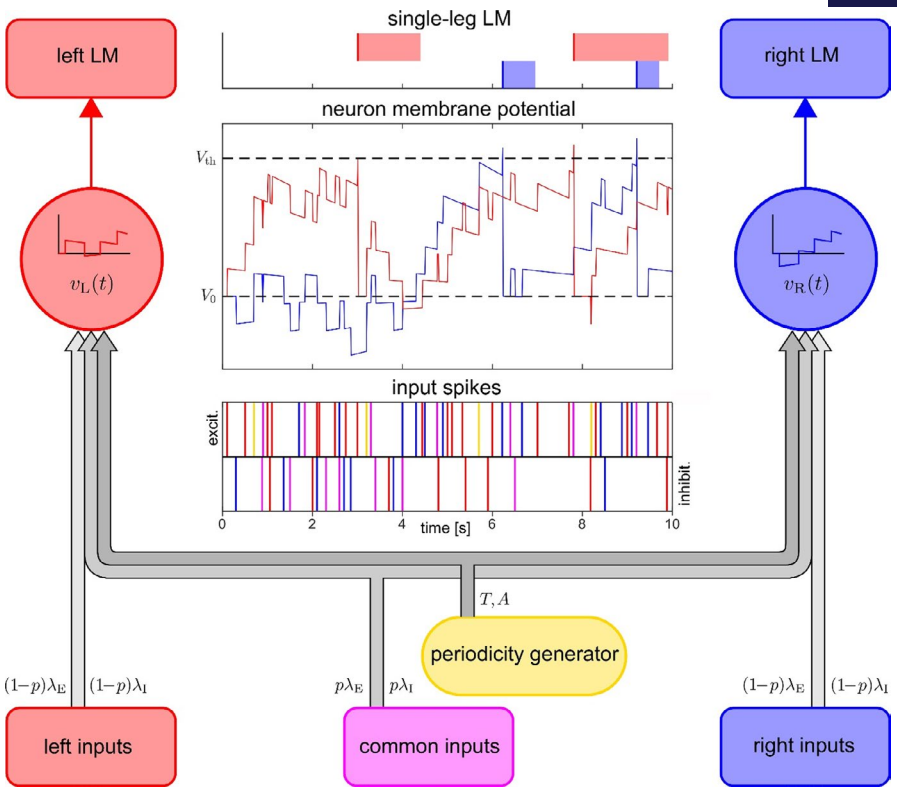

FIGURE 1 Schematic representation of the model. The left and right motor neurons (red and blue circular nodes) implement the integrate-and-fire model, with membrane potentials *v*L(*t*) and *v*R(*t*) at time *t* and same rest potential *V*0 and fire threshold *V*th. Leg-specific and common physiological inputs from the central nervous system (CNS; red, blue and magenta rectangular source nodes) are modelled by spikes of synaptic current causing steps of equal amplitude *a* in the membrane potentials (positive/negative steps for excitatory/inhibitory spikes; Poissonian arrival rates are indicated next to the input arrow). The single periodicity generator (gold) produces a *T*-periodic train of excitatory spikes with potential step amplitude *A*. If t_k and t_{k+1} are the arrival times of two consecutive spikes (not necessarily of the same type) and $v_X(t_k)$ is the membrane potential reached by the neuron just after the contribution of the *k*-th spike (X = L, R), the potential evolution in the time interval t_k, t_{k+1} [up to but not including the contribution of the (*k*+1)-th spike] is an exponential decay toward V_0 with time-constant τ (see Eq. [S2]). At the arrival of the (*k*+1)-th input spike, the decayed potential at time t_{k+1} is updated by adding/subtracting the spike contribution. This results in the simulation scheme detailed in Section S1

TABLE 1 Summary of the model parameters and their calibration

Parameter	Value/distribution (μ σ)			Description
V_0		0		Neuron membrane resting potential
V_{th}		1		Neuron membrane threshold potential
a		0.1		Amplitude of physiological input spikes
LM duration	Non-parametric	2.47	2.43	LM duration
λ_E	GEV	4.73	3.14	Arrival rate of excitatory input spikes
λ_I	N	$1.031\lambda_E + 0.118 + 0.002\,\lambda_E{}^2$	0.05	Arrival rate of inhibitory input spikes
p	Beta	0.93	0.07	Proportion of common inputs
T	GEV	24.42	5.16	Period of the periodicity generator
A	LogN	0.72	0.60	Amplitude of the periodic input spikes

Abbreviations: GEV, generalized extreme value; LM, leg movement.

the periodicity generator are patient-specific and describe the disease severity.

As typical when using the integrate-and-fire neuron model, we describe the physiological inputs as a series of synaptic current spikes, with Poisson-distributed arrival times, each causing the membrane potential to instantaneously step up or down by a small amount controlled by parameter *a*. We denoted by λ_E and λ_I the arrival rates – average number of spikes per second – of excitatory (E)

and inhibitory (I) inputs, divided into common (rates $p\,\lambda_E$ and $p\,\lambda_I$) and leg-specific (same rates $(1-p)\,\lambda_E$ and $(1-p)\,\lambda_I$ for both legs; Figure 1). The three arrival processes (common and left-/right-specific) are independent. The periodicity generator is also assumed to produce a series of synaptic current spikes, with period *T*, each spike causing an upward potential step controlled by parameter *A*.

2.2 | Calibration

Table 1 summarizes the list of the model parameters, together with their calibrated values; for those that are subject-specific, the mean and standard deviation of the identified probability distributions are reported (see Section S2 for details on the calibration procedures). Dataset summary information is provided in Section S3 (including ethical approval statement). All parameters were supposed to remain constant during the simulation period.

Parameters V_0, V_{th} and a are essentially scaling parameters and do not need calibration (see Section S2.1). We set $V_0 = 0$, $V_{th} = 1$ and $a = 0.1$ (10% of the rest-to-fire interval). This conventional choice, however, affects the calibration of the arrival rates λ_E and λ_I.

The duration of single-LMs was fitted on all LM durations recorded in the noPLMs dataset (32 subjects characterized by normal PLMs and unimodal IMI distribution, mean age 48.03 years [SD 20.75] and 56.25% women; see Section S3). Because no common parametric distribution showed statistical agreement with the LM duration data, we used a non-parametric technique (kernel density estimation; Ferri et al., 2006; Gramacki, 2018; see Section S2.2). According to the resulting distribution, we independently obtained the duration of all simulated LMs at the movement onset (i.e. at the firing of the leg neuron). Because no significant correlation is documented between the subjects' LM duration and PLM index, we used the same distribution to generate also the LM durations of virtual PLM subjects. This choice is in line with the primary aim of the study.

The arrival rates λ_E and λ_I of physiological input spikes, the proportion parameter p between common and leg-specific inputs, and the membrane time constant τ characterize noPLM subjects and were calibrated using the noPLM dataset (see Sections S2.3–S2.5). The result is a τ-dependent statistical fitting for λ_E, λ_I and p, that we used to generate a virtual population of noPLM subjects. Specifically, we calibrated τ to match the shape of the IMI distribution observed in the noPLM dataset. The corresponding distributions identified for λ_E and p turned out to be a generalized extreme value (GEV) and a Beta. For the rate of inhibitory inputs λ_I, we identified a nearly linear correlation with λ_E.

The distributions of the two parameters, period *T* and amplitude *A*, of the periodicity generator were then fitted using the PLM dataset (65 subjects, mainly affected by RLS, characterized by abnormal PLM index and bimodal IMI distribution, mean age 58.52 years [SD 13.09] and 66.15% women; see Section S3). The period sample distribution was built by visual inspection, looking at the second peak of the subject's IMI distribution (Section S2.6), which is known to characterize the temporality of the PLM phenomenon (Ferri et al., 2006). The corresponding sample of amplitude *A* was optimized to match, on average, the subject's LM index (Section S2.7). The sample distributions of *T* and *A* were best fitted by a GEV and a LogNormal distribution, respectively.

Note the twofold use of the statistical fitting for λ_E, λ_I and p. They were used to generate several τ -dependent virtual populations of noPLM subjects during the calibration of the time constant τ and also, for the calibrated value of τ, to generate single subject profiles for the calibration of the amplitude *A* of the periodicity generator. Indeed, recall that a virtual PLM subject is obtained by simply adding the periodicity generator to a noPLM profile.

2.3 | Statistics

To validate our model, we compared the principal indicators derived from the real and simulated LM activity at the population level (one sample for each real and each virtual subject). We tested the LM index (number of LMs per hr), the PLM index (number of PLM per hr), the periodicity index (PI = PLM index/LM index), and short-, mid- and long-IMI indexes (hourly number of CLMs with IMI < 10 s, within the range 10–90 s, and > 90 s; Table 2). We also included in the comparison the principal features of monolateral and bilateral LMs (Table 3). For each indicator, we looked at the Cohen's *d* effect size, a measure (based on means difference) of the discrepancy between the real and the simulated data (0.2–0.5–0.8 is indicative of a small–medium–large effect size). Moreover, we considered the 95% confidence interval (CI) of the indicator sample mean on both real and simulated data, and we computed their overlap. Finally, to show the goodness of the model as a generator of in-silico data, we used the Mann–Whitney *U*-test to statistically test the hypothesis that real and simulated data come from the same probability distribution.

3 | RESULTS

Tables 2 and 3 summarize the main LM features in real and simulated data, together with their comparison (see Section S1 for the detailed selection and simulation procedures for virtual noPLM and PLM subjects). We found small effect size, good CI overlap, and no statistically significant differences between real and simulated data for LM index, short-IMI index and mid-IMI index for both noPLM and PLM subjects (Table 2). On the contrary, data differed significantly in PLM index and PI, for both noPLM and PLM subjects, and in long-IMI index, for PLM subjects only (Table 2). Incidence and characteristics of monolateral and bilateral LMs were generally similar between real and simulated data, for both noPLM and PLM subjects (Table 3), with the exception of the max bilateral LM duration, for PLM subjects.

Figure 2 shows the IMI distributions of the noPLM (top panels) and PLM (bottom panels) groups, for both real (left) and simulated (right) data; a higher number of long IMIs is clearly evident in the comparison between real and simulated PLM data, in agreement with the findings reported in Table 2.

TABLE 2 LM features in real and virtual (simulated) noPLM and PLM subjects

	Recording		Simulation		Statistics		
	Mean (SD)	95% CI	Mean (SD)	95% CI	*p*-value	Cohen's *d*	CI overlap (%)
noPLM subjects (32)							
LM index	13.44 (6.29)	11.3–15.6	13.54 (6.38)	11.3–15.8	0.957	0.016	95.6
CLM index	12.88 (5.58)	11.0–14.8	13.00 (6.12)	10.9–15.1	0.804	0.022	90.5
PLM index	1.54 (1.59)	0.99–2.09	0.65 (0.73)	0.40–0.91	0.019	−0.719	0
PI	0.13 (0.14)	0.08–0.18	0.04 (0.05)	0.02–0.06	0.005	−0.856	0
Short-IMI index	2.71 (2.15)	1.96–3.46	2.84 (1.66)	2.26–3.42	0.468	−0.034	77.3
Mid-IMI index	4.89 (2.71)	3.95–5.83	4.40 (2.34)	3.59–5.21	0.658	−0.324	56.3
Long-IMI index	4.55 (1.75)	3.94–5.16	5.02 (1.70)	4.43–5.61	0.405	0.291	45.5
PLM subjects (65)							
LM index	56.90 (46.22)	45.7–68.1	60.69 (45.15)	49.7–71.7	0.328	0.082	70.8
CLM index	55.31 (42.67)	44.9–65.7	57.52 (42.21)	47.2–67.8	0.565	0.052	80.8
PLM index	29.17 (19.78)	24.4–30.0	14.21 (22.1)	8.66–19.8	< 0.001	−0.701	0
PI	0.55 (0.20)	0.49–0.60	0.25 (0.21)	0.19–0.30	< 0.001	−1.463	0
Short-IMI index	12.45 (24.69)	6.45–18.4	17.15 (11.67)	14.3–20.0	0.257	0.243	30.3
Mid-IMI index	37.12 (22.10)	31.7–42.5	35.08 (31.61)	27.4–42.8	0.390	−0.076	70.1
Long-IMI index	4.05 (1.76)	3.62–4.48	8.58 (2.85)	7.89–9.27	< 0.001	1.913	0

Statistical comparison by means of the Mann–Whitney *U*-test, the Cohen's *d* effect size, and the sample mean CI overlap.

Abbreviations: CI, confidence interval; CLM, candidate leg movement; IMI, inter-movement interval; LM, leg movement; PI, periodicity index; PLM, periodic limb movement.

Finally, Figure 3 shows a 5-min example of an in-silico LM series generated by a randomly selected virtual PLM subject.

4 | DISCUSSION

Leg movements during sleep and, in particular, their periodic portion, are under the attention of clinical researchers for their potential repercussions on the health status of patients suffering from conditions associated to them, such as RLS in the first place (Ferri, 2012). There is little doubt that this motor phenomenon is associated with significant electroencephalographic and cardiovascular transient changes which, when repeated every night for years, might lead to a series of neurological and cardiovascular sequelae. However, the assessment of their real clinical meaning is still under debate, and made difficult by their inter-individual and intra-individual (nigh-to-night) variability (Ferri et al., 2017; Figorilli et al., 2017). In this perspective, the arrangement of a reliable model of PLMs would be welcome by the scientific community because of the possibility to better control their variability and put forward hypotheses and, maybe, new ideas for their assessment and treatment.

Our calibrated model can be used to generate and simulate virtual (in-silico) populations of both noPLM and PLM subjects. We chose to create populations of size equal to the corresponding datasets used for the model calibration (32 noPLM and 65 PLM subjects), and we compared the typical features calculated on the simulated LM data with those obtained from real PSG data.

A limitation of this study is that we used for the assessment of the model performance the same datasets available for calibration. However, our model is not aimed at forecasting the LM activity of new subjects. Our primary aim was to test the single-generator hypothesis behind PLMs, a goal for which the dataset splitting into calibration and validation is not necessary. Moreover, the comparison was not done at the level of the single subject, but at group level. Indeed, we used the data on the real LM activity not to reproduce the real patients, but to calibrate the distributions of the model parameters from which we randomly generated groups of virtual subjects. This made the comparison between the average LM activity in the real and virtual populations reliable.

Remarkably, the small effect size and good CI overlap among real and simulated data validate our model for both noPLM and PLM subjects. Moreover, the absence of a statistical difference between real and simulated data confirms the good performance of the model. As expected, the agreement is very evident for the monolateral LM features of the noPLM group, as the distribution of LM duration is fitted on all single-LMs in the noPLM dataset (see calibration in Section 2.2). Remarkably, we did not find significant differences either for the bilateral LM features; this further supports the goodness of the model for noPLM subjects.

TABLE 3 Monolateral and bilateral LM features in real and virtual (simulated) noPLM and PLM subjects

	Recording		Simulation		Statistics		
	Median (IQR)	95% CI	Median (IQR)	95% CI	*p*-value	Cohen's *d*	CI overlap (%)
noPLM subjects (32)							
Bilateral LM							
# single LM, min	2.0 (2.00–2.00)	2.00–2.00	2.0 (2.00–2.00)	2.00–2.00	1	—	100
Max	3.0 (2.00–3.00)	2.52–3.10	3.0 (2.00–3.00)	2.41–2.83	0.916	0	44.9
Median	2.0 (2.00–2.00)	2.00–2.00	2.0 (2.00–2.00)	2.00–2.00	1	—	100
Duration (s), min	1.01 (0.82–1.13)	0.92–1.14	0.96 (0.81–1.22)	0.99–1.48	0.973	0.323	26.8
Max	9.19 (8.26–9.69)	8.27–9.21	9.67 (8.37–11.8)	8.81–10.2	0.134	0.356	21.2
Median	3.34 (2.98–3.91)	3.21–3.87	3.28 (2.85–3.74)	3.12–3.68	0.462	0.147	54.7
Bilateral LM (%)	31.4 (23.5–40.0)	28.9–39.4	30.9 (15.4–43.7)	24.8–33.7	0.875	0.034	33.1
Monolateral LM							
Duration (s), min	0.53 (0.51–0.57)	0.52–0.64	0.52 (0.51–0.55)	0.51–0.55	0.918	0.096	23.1
Max	8.50 (6.42–9.72)	7.04–8.56	8.69 (7.53–9.29)	7.77–8.67	0.655	0.087	48.5
Median	1.59 (1.29–1.70)	1.41–1.65	1.54 (1.46–1.69)	1.46–1.61	0.468	0.147	62.5
PLM subjects (65)							
Bilateral LM							
# single LM, min	2.0 (2.00–2.00)	2.00–2.00	2.0 (2.00–2.00)	2.00–2.00	1	—	100
Max	3.0 (3.00–4.00)	2.94–3.44	4.0 (3.00–4.00)	3.24–3.66	0.131	0.235	27.8
Median	2.0 (2.00–2.00)	2.00–2.00	2.0 (2.00–2.00)	2.00–2.00	1	—	100
Duration (s), min	0.92 (0.73–1.10)	0.89–1.06	0.83 (0.73–1.22)	0.93–1.11	0.115	−0.299	59.1
Max	9.71 (9.47–9.91)	9.42–9.72	12.9 (11.5–13.8)	12.2–13.4	< 0.001	2.129	0
Median	3.32 (2.84–3.96)	3.23–3.61	3.18 (2.86–3.74)	3.10–3.33	0.118	0.182	19.6
Bilateral LM (%)	39.6 (28.1–53.9)	37.5–47.6	37.6 (29.9–50.5)	37.4–44.6	0.697	0.098	69.6
Monolateral LM							
Duration (s), min	0.51 (0.51–0.53)	0.51–0.55	0.51 (0.51–0.52)	0.51–0.53	0.594	0	50.0
Max	9.30 (7.35–9.77)	8.00–8.84	9.42 (8.78–9.74)	8.54–9.28	0.431	0.120	23.4
Median	1.69 (1.40–2.14)	1.67–1.93	1.51 (1.42–1.57)	1.45–1.75	0.227	−0.477	16.6

Statistical comparison as in Table 2.

Abbreviations: CI, confidence interval; IQR, interquartile range; LM, leg movement; PLM, periodic limb movement.

Regarding PLM subjects, we similarly found a good agreement (small effect size and good CI overlap; no significant statistical difference) between real and simulated data for both the monolateral and bilateral LM features. In particular, the model well captures the increase of the proportion of bilateral LMs in PLM subjects. These results provide preliminary support for the view of the single periodicity generator.

Conversely, significant differences were found for the parameters requiring some temporal structure among LMs. This is the case of the PLM index (Ferri et al., 2016) and PI (Table 2). The PLM index considers only sequences of at least four consecutive CLMs separated by IMIs of between 10 s and 90 s, and interrupted by either a non-candidate LM or an IMI out of the range 10–90 s. The reason for the disagreement is therefore rooted in the stationarity of the model parameters during the simulated night, in contrast to the different time structure of the real LM activity expressed during the different sleep stages and wakefulness. Indeed, looking at the numbers of IMIs in each of the three characteristic intervals, i.e. < 10 s (short-IMI, characteristic of noPLM individuals), 10–90 s (mid-IMI characteristic of PLM subjects) and > 90 s (long-IMI), without requiring sequencing, we found good agreement between recorded and simulated data (see Table 2, last block of rows). Only the number of long-IMIs is larger in our simulations, but this is, again, to be considered an artefact of the model stationarity. Indeed, there is evidence that PLMs decrease along the night (Ferri, 2012), so that mid-IMIs are concentrated at the beginning of the night. However, calibrating a stationary periodicity generator that matches, on average, the number of real LMs (see 'Calibration') gives several long IMIs in lieu of few very long ones, the latter corresponding to night phases with essentially no LM activity; the number of long-IMIs is therefore overestimated.

4.1 | Future research

It is always difficult to establish the value of a first in-silico model of a physiopathological phenomenon, such as PLMs, and to predict the possible future use of such a model. However, in order to at

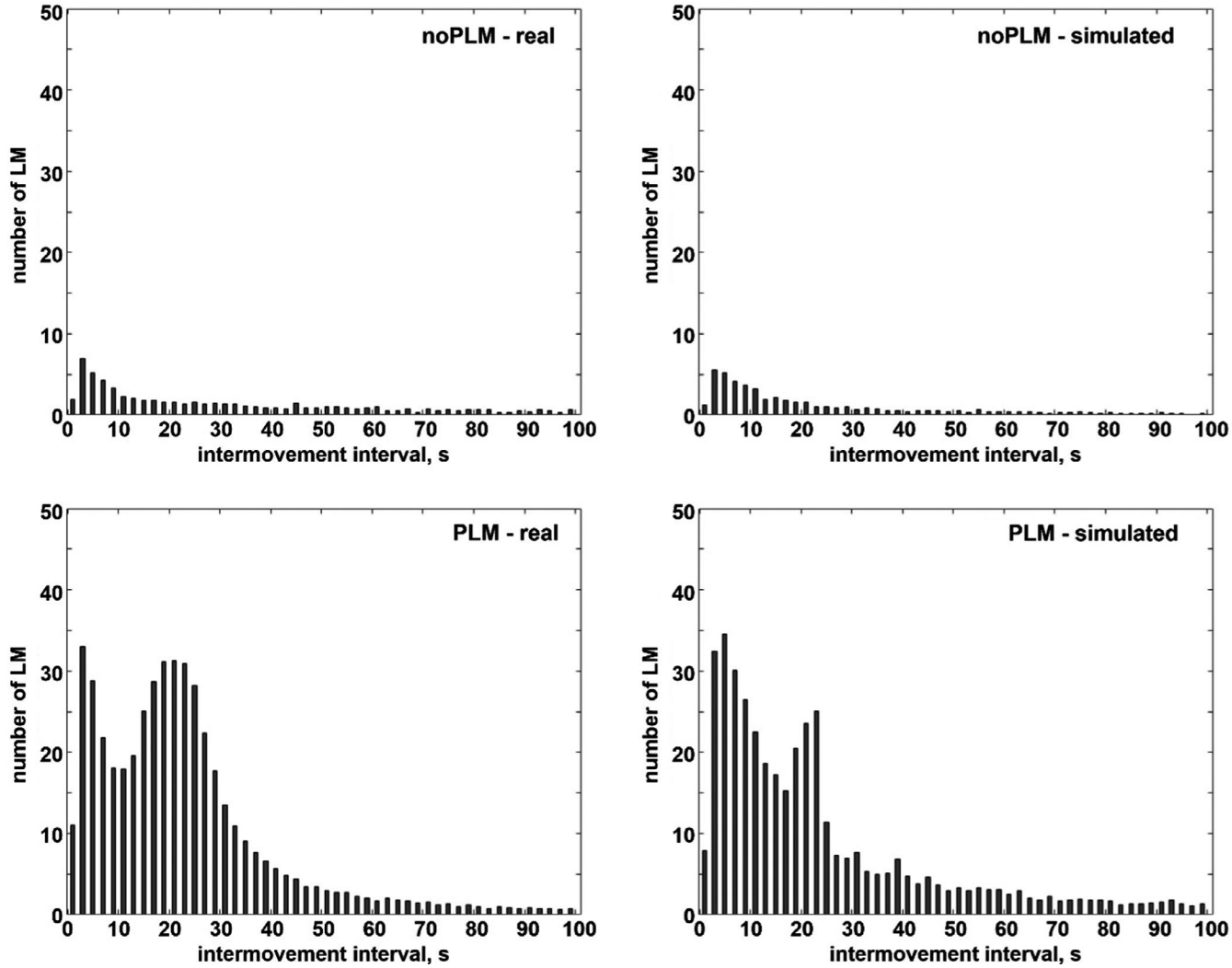

FIGURE 2 Inter-movement interval (IMI) distribution in noPLM real (top-left panel) and simulated (top-right panel) subjects, and in PLM real (bottom-left panel) and simulated (bottom-right panel) subjects. PLM, periodic limb movement

least partially address this concern, we have tried to speculate on possible future applications of our model. If this model will be confirmed to be able to simulate realistically the time structure of true PLMs, it might be practically useful for the following purposes.

- Developing more complex and realistic models that can answer critical and clinical questions. For example, by including cortical and autonomic oscillations in the future models, it will be possible to better understand the relationship between these systems.
- Understanding the complexity of the network behind the periodicity of PLMs.
- Produce countless simulations of virtual recordings, reducing the high costs associated with PSG and the relative burden for the patients.
- Simulate the effect of external interventions (perturbations) on the system, such as the effect of particular drugs on PLMs, thus improving safety for patients potentially exposed to side-effects. For instance, by comparing the results between recordings after administration of DAs in real patients and the virtual data, after switching off the virtual oscillator, we might help understanding if DAs act by turning off the periodic generator or by working on another network. Similarly, we can compare the two datasets in other pharmacological contexts, such as using published data on the effect of sedatives that we know have a scarce effect on PLMs.
- The parameters "*A*" (oscillator amplitude) and "*T*" (oscillator period) could be used as new indicators of the "severity" and "temporality" of PLMs, respectively, to be used in parallel with the recently introduced parameters, like the "PI".
- Considering also the patients' metadata, it will be possible to perform cluster analyses for the model parameters, favouring the important and still missing mission of PLM phenotyping.

5 | CONCLUSION

Recalling that, in our model, a virtual PLM subject is nothing but a virtual noPLM subject with the addition of the periodicity generator,

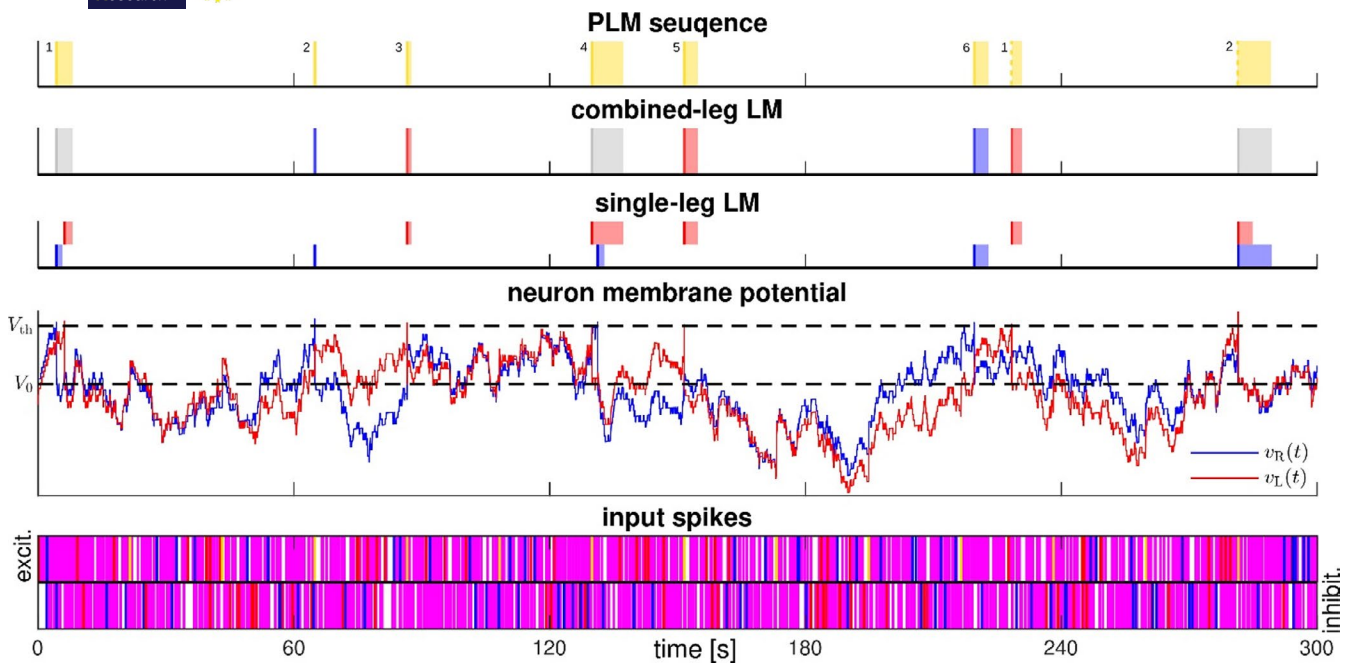

FIGURE 3 Example of a 5-min in-silico leg movement (LM) activity. Input spikes: leg-specific physiological inputs, left (red) and right (blue); common physiological input (magenta); periodicity generator (gold). Neuron membrane potential: left (red) and right (blue) neurons. Single-leg LM: onset (solid bar) and duration (shaded area) of left (red) and right (blue) LM. Combined-leg LM: monolateral LM (red and blue); bilateral LM (grey). Periodic limb movement (PLM) sequence: numeric labels progressively count candidate leg movement (CLM) in a potential PLM sequence (composed of min 4 CLMs). The sequence of 6 PLMs (gold) is interrupted by a short inter-movement interval (IMI; < 10 s); the two following LMs are CLMs (dashed gold bar); they will be counted as PLMs if the sequence reaches 4. Simulated data obtained with parameters $\lambda_E = 2.76$, $\lambda_I = 3.04$, $p = 0.95$, $T = 21.66$ and $A = 0.55$ of a randomly extracted virtual PLM subject (Table 1)

and that the generator is calibrated by fitting LM indexes, rather than PLM indicators, we conclude that the agreement we found between real and simulated data supports the single-generator hypothesis behind PLMs.

Indeed, the Cohen's *d* effect size between the indicators calculated on real and simulated data and the overlap between the CI of the indicators sample means validate the model (Tables 2 and 3). Moreover, the absence of a statistically significant difference between real and simulated LM features, the incidence of bilateral LMs in particular, is evidence of a good performance.

The quantitative agreement was not obtained on the indicators requiring a temporal structure among LMs (PLM index and PI). This, however, does not contradict our conclusion, because the disagreement is well explained by the simplicity of the model – the parameters stationarity in particular – which, in turn, is what makes our model appealing.

Overall, the results exposed in this paper are definitely encouraging and represent a solid basis for the refinement of the model here presented. In particular, with more data available (including several recordings for each subject), specific calibrations could be obtained for the different sleep stages and during wakefulness, aiming at a more quantitative model ready for clinical applications.

ACKNOWLEDGMENTS

We thank the anonymous reviewers for their careful reading and constructive suggestions. We also acknowledge the positive feedback obtained from the reviewers and participants of the International Conference on Computational Intelligence Methods for Bioinformatics and Biostatistics, CIBB 2021, where a preliminary version of this work has been presented.

CONFLICT OF INTEREST

No conflict of interest has been declared by the authors.

DATA AVAILABILITY STATEMENT

Data sharing not applicable – no new data generated.

ORCID

Matteo Italia https://orcid.org/0000-0001-9633-8396
Fabio Dercole https://orcid.org/0000-0001-9256-0651
Raffaele Ferri https://orcid.org/0000-0001-6937-3065
Mauro Manconi https://orcid.org/0000-0002-1849-7196

REFERENCES

Allen, R. P., Donelson, N. C., Jones, B. C., Li, Y., Manconi, M., Rye, D. B., Sanyal, S., & Winkelmann, J. (2017). Animal models of RLS phenotypes. *Sleep Medicine*, *31*, 23–28. https://doi.org/10.1016/j.sleep.2016.08.002

American Academy of Sleep Medicine. (2014). *International classification of sleep disorders* (3rd ed.). American Academy of Sleep Medicine.

Burkitt, A. N. (2006). A review of the integrate-and-fire neuron model: I. Homogeneous synaptic input. *Biological Cybernetics*, *95*, 1–19. https://doi.org/10.1007/s00422-006-0068-6

Ferri, R. (2006). Two legs, one heart, one sleeping brain. *Nature Communications*, *7*(3), 299–300. https://doi.org/10.1016/j.sleep.2005.10.001

Ferri, R. (2012). The time structure of leg movement activity during sleep: The theory behind the practice. *Sleep Medicine*, *13*(4), 433–441. https://doi.org/10.1016/j.sleep.2011.10.027

Ferri, R., Fulda, S., Allen, R., Zucconi, M., Bruni, O., Chokroverty, S., Ferini-Strambi, L., Frauscher, B., Garcia-Borreguero, D., Hirshkowitz, M., Högl, B., Inoue, Y., Jahangir, A., Manconi, M., Marcus, C., Picchietti, D., Plazzi, G., Winkelman, J. W., & Zak, R. (2016). World association of sleep medicine (WASM) 2016 standards for recording and scoring leg movements in polysomnograms developed by a joint task force from the international and the European restless legs syndrome study groups (IRLSSG and EURLSSG). *Sleep Medicine*, *26*, 86–95. https://doi.org/10.1016/j.sleep.2016.10.010

Ferri, R., Koo, B. B., Picchietti, D. L., & Fulda, S. (2017). Periodic leg movements during sleep: Phenotype, neurophysiology, and clinical significance. *Sleep Medicine*, *31*, 29–38. https://doi.org/10.1016/j.sleep.2016.05.014

Ferri, R., Proserpio, P., Rundo, F., Lanza, A., Sambusida, K., Redaelli, T., De Carli, F., & Nobili, L. (2015). Neurophysiological correlates of sleep leg movements in acute spinal cord injury. *Clinical Neurophysiology*, *126*(2), 333–338. https://doi.org/10.1016/j.clinph.2014.05.016

Ferri, R., Zucconi, M., Manconi, M., Plazzi, G., Bruni, O., & Ferini-Strambi, L. (2006). New approaches to the study of periodic leg movements during sleep in restless legs syndrome. *Sleep*, *29*(6), 759–769.

Figorilli, M., **Puligheddu**, M., **Congiu**, P., & **Ferri**, R. (2017). The clinical importance of periodic leg movements in sleep. *Current Treatment Options Neurology*, *19*(3), 10. https://doi.org/10.1007/s11940-017-0446-5

Gramacki, A. (2018). *Nonparametric kernel density estimation and its computational aspects*. Springer. https://link.springer.com/book/10.1007/978-3-319-71688-6

Manconi, M., Ferri, R., Zucconi, M., Bassetti, C. L., Fulda, S., Aricò, D., & Ferini-Strambi, L. (2012). Dissociation of periodic leg movements from arousals in restless legs syndrome. *Annals of Neurology*, *71*(6), 834–844. https://doi.org/10.1002/ana.23565

Manconi, M., Ferri, R., Zucconi, M., Oldani, A., Fantini, M. L., Castronovo, V., & Ferini-Strambi, L. (2007). First night efficacy of pramipexole in restless legs syndrome and periodic leg movements. *Sleep Medicine*, *8*(5), 491–497. https://doi.org/10.1016/j.sleep.2006.10.008

Pennestri, M. H., Whittom, S., Adam, B., Petit, D., Carrier, J., & Montplaisir, J. (2006). PLMS and PLMW in healthy subjects as a function of age: Prevalence and interval distribution. *Sleep*, *29*(9), 1183–1187. https://doi.org/10.1093/sleep/29.9.1183

Salminen, V., Manconi, M., Rimpilä, V., Luoto, T. M., Koskinen, E., Ferri, R., Ohman, J., & Polo, O. (2013). Disconnection between periodic leg movements and cortical arousals in spinal cord injury. *Journal of Clinical Sleep Medicine*, *9*(11), 1207–1209. https://doi.org/10.5664/jcsm.3174

Stein, R. B. (1965). A theoretical analysis of neuronal variability. *Biophysical Journal*, *5*(2), 173–194. https://doi.org/10.1016/S0006-3495(65)86709-1

SUPPORTING INFORMATION

Additional supporting information may be found in the online version of the article at the publisher's website.

How to cite this article: Italia, M., Danani, A., Dercole, F., Ferri, R., & Manconi, M. (2022). A calibrated model with a single-generator simulating polysomnographically recorded periodic leg movements. *Journal of Sleep Research*, 00, e13567. https://doi.org/10.1111/jsr.13567